





# Deep Learning Aided Minimum Mean Square Error Estimation of Gaussian Source in Industrial Internet-of-Things Networks

Majumder Haider , Graduate Student Member, IEEE, Md. Zoheb Hassan , Member, IEEE, Imtiaz Ahmed , Senior Member, IEEE, Jeffrey H. Reed , Life Fellow, IEEE, Ahmed Rubaai, Life Fellow, IEEE, and Danda B. Rawat , Senior Member, IEEE

Abstract—This article investigates the problem of estimating complex-valued Gaussian signals in an industrial Internet of Things (IIoT) environment, where the channel fading is temporally correlated and modeled by a finite state Markov process. To address the non-trivial problem of estimating channel fading states and signals simultaneously, we propose two deep learning (DL)-aided minimum mean square error (MMSE) estimation schemes. More specifically, our proposed framework consists of two steps, (i) a DL-aided channel fading state estimation and prediction step, followed by (ii) a linear MMSE estimation step to estimate the source signals for the learned channel fading states. Our proposed framework employs three DL models, namely the fully connected deep neural network (DNN), long short-term memory (LSTM) integrated DNN, and temporal convolution network (TCN). Extensive simulations show that these three DL models achieve similar accuracy in predicting the states of wireless fading channels. Our proposed data-driven approaches exhibit a reasonable performance gap in normalized mean square error (NMSE) compared to the genie-aided scheme, which considers perfect knowledge of instantaneous channel fading states.

Index Terms—Channel fading, deep learning, Internet of Things (IIoT), Industry 5.0, minimum mean square error (MMSE), Markov process.

### I. INTRODUCTION

# A. Introductory Background

NDUSTRIAL Internet-of-things (IIoT) networks pave the way for wireless control, monitoring, and process automation by implementing machine-to-machine (M2M) communications

Manuscript received 24 October 2023; revised 2 March 2024 and 27 March 2024; accepted 22 June 2024. Date of publication 1 July 2024; date of current version 12 July 2024. This work was supported in part by National Science Foundation (NSF) Project under Award 2200640, in part by Intel Corporation, in part by DoD/US Army Contract W911NF-20-2-0277, and in part by DoD/US Army Contract W911NF-22-1-0224. (Corresponding author: Majumder Haider.)

Majumder Haider, Imtiaz Ahmed, Ahmed Rubaai, and Danda B. Rawat are with the Department of EECS, Howard University, Washington, DC 20059 USA (e-mail: majumder.haider@bison.howard.edu).

Md. Zoheb Hassan is with the Department of Electrical and Computer Engineering, Université Laval, Quebec City, QC G1V 0A6, Canada. Jeffrey H. Reed is with the Wireless@VT, Bradley Department of ECE,

Virginia Tech, Blacksburg, VA 24061 USA.

Digital Object Identifier 10.1109/TICPS.2024.3420823

in the industrial environment [1]. In today's industrial environments, IIoT solutions can lead to the development of creative and efficient systems aimed at enhancing business operational efficiency in a new generation of smart factories such as Industry 4.0 [2]. The evolving IIoT technology extends the vision of large-scale M2M communications through the seamless convergence of smart distributed control systems technology and intelligent human-machine interfaces (HMIs). IIoT network is expected to automate the entire supply chain and production by providing ubiquitous access to real-time information while ensuring scalability and security of information aggregation utilizing augmented reality (AR) technology [3].

In the IIoT networks, accurate detection of the signals transmitted from various sensors, controllers, and actuators is of paramount importance for analyzing data and making rapid process control decisions. However, unlike terrestrial wireless communications, IIoT networks exhibit a hostile communication environment consisting of large metal objects, moving machines, vehicles, and various radio emitters [4]. In particular, the dynamic variation of the industrial environment, caused by signal reflection from metallic surfaces, moving objects, and frequent location changes of equipment, leads to spatially and temporally correlated channel fading [5], [6]. Furthermore, the transmitted signal is also corrupted by bursty impulsive noise generated by the power equipment, machine tools, and radio emitters in the industrial environment [6]. Because of such channel impairments, accurate signal detection in the IIoT environment is a non-trivial problem and the conventional linear minimum mean square error (LMMSE) technique fails to provide optimal results. LMMSE is optimal in the minimum mean square error (MMSE) sense when the signal is impaired by only Gaussian noise, for example, when the signal is transmitted over a time-invariant channel with deterministic channel gain. However, in the presence of spatially and temporally correlated channel fading and bursty impulsive noise, the relationship between the input and output signals of a communication channel deviates from a simple linear relationship. Consequently, the conventional LMMSE is no longer effective for source signal estimation in IIoT networks. The non-linear characteristics of the signals become mathematically intractable using the conventional LMMSE approach. In this circumstance, deep learning (DL) can shed light to exploit the non-linear characteristics

2832-7004 © 2024 IEEE. Personal use is permitted, but republication/redistribution requires IEEE permission. See https://www.ieee.org/publications/rights/index.html for more information.

of the signals efficiently by intelligently analyzing the spatial correlation in the data of the fading channel states.

This work studies the problem of detecting complex-valued Gaussian signals transmitted in IIoT networks by employing the MMSE technique, where the transmitted signals are subjected to Markov channel fading with a finite number of states. In timecorrelated fading channels, conventional MMSE estimators exhibit sub-optimal mean square error (MSE) performance, and the computational complexity of the optimal MMSE estimator grows exponentially with frame sizes [6]. To tackle the challenge of near-optimal MMSE estimation with low computational complexity, we investigate the applicability of multiple data-driven signal estimation approaches by employing different deep neural network (DNN) techniques. We propose a two-step data-driven approach. More precisely, at first, we employ DL methods to estimate channel fading states, and subsequently, an LMMSE estimator is leveraged to estimate signals for the learned channel fading states. We develop two DL-aided methods for estimating and predicting channel fading states. The superiority of the proposed DL approaches over benchmark schemes is verified via extensive simulations.

### B. Related Work

The cellular industry has prioritized industrial automation as a potential market for its products and is committed to taking these requirements into account in parallel to the development of fifthgeneration (5G) and beyond networks [7]. Additionally, digital renovation such as network virtualization and semantic communications with the advancement of artificial intelligence (AI) has great potential to alter the structure of industrial networks and can play a crucial role in facilitating the goals of IIoT [8], [9]. The rapid progress of wireless technologies, their greater flexibility in deployment, and easy move-out due to having no cables make them a prominent choice to bring revolutionary changes in industry automation replacing the wired technologies that have been established in past decades [10], [11]. Although interference, multipath fading, delay sensitivity, and intermittent connectivity issues pose challenges for reliable wireless communications, the concept of the Internet of Everything (IoE) transforms the traditional wired technology into a wireless solution in order to facilitate the goals of Industry 4.0 [12], [13].

The fading distribution of wireless channels has a greater effect on transmission accuracy, delay sensitivity, and energy-efficient communications [5], [14]–[16]. We emphasize that the channel fading in the practical IIoT networks shows temporal correlations [5]. Moreover, the probability density function (PDF) of channel fading in IIoT networks is typically modeled as a mixture distribution [5], [17], [18]. As such channel fading possesses different states to have different fading distributions, and the correlation among these states controls the memory of the fading channel [5], [15], [17]. In this model, the mixing probability represents the percentage of time during which the channel fading adheres to a specific component distribution over an arbitrarily long period of operation. Combining these two properties, we conclude that the channel fading process of an IIoT network can be effectively modeled by a finite

state Markov chain with memory. Such a modeling approach is particularly suitable for IIoT networks since (i) it captures the inherent temporal correlation among different channel fading states and (ii) the steady-state probability of the Markov chain becomes the same as the mixing probability of the mixture fading distribution. Accordingly, we exploit the Markov chain to model the transition among different fading states. It is noteworthy that the considered finite-state Markov fading model in our work can capture both memories in the channel fading and the variability of states over a certain time duration.

### C. Motivations and Contributions

Although this work is motivated by the initial results obtained in [19], the system model and the design objectives of this work are fundamentally different from [19]. There are two unique differences between the system models considered in this work and in [19] and [20]. First, in this work, we consider that the transmit signal is impaired by temporally-correlated and frequency-flat fading channels. In contrast, the system models of [19] and [20] did not consider any fading channels. Second, this work considers additive white Gaussian noise (AWGN) at the receiver, whereas the underlying noise considered in [19] and [20] was two-state Markov Gaussian noise. We emphasize that the aforementioned system model differences are due to different objectives of the current and previous works. Specifically, the objective of the current work is to develop a suitable method to accurately estimate the Gaussian distributed signal transmitted by the source, which is impaired by the fading channels in IIoT networks. To effectively model channel impairment that exhibits temporal correlation in IIoT networks, this work considers a Markov fading channel with finite numbers of fading states and memory, where different states of the considered fading channel can have different fading distributions. In contrast, the key objective of [19] and [20] was the accurate estimation of the Gaussian distributed signal source, which is impaired by an additive impulsive non-Gaussian noise. More specifically, both [19] and [20] considered a fading-less environment with two-state Markov Gaussian noise. Therefore, although both the present work and existing [19] and [20] study the problem of estimating Gaussian distributed source signals, their considered system models are entirely different.

Although digital communication signals can deviate from Gaussian distributions in the practical field, there are certain industry applications where the signals possess Gaussian distributions [21], [22]. It is worth noting that when different fading states take different deterministic values instead of a fading distribution and the transmitted signal is Gaussian, the LMMSE becomes the optimal MMSE estimator of the signal for a given fading state. Nevertheless, such an optimal MMSE estimator does not necessarily exploit the temporal correlation structure of the channel fading and therefore, exhibits degraded estimation accuracy when the fading channel has a large memory or correlation among its states [20]. In fact, when the fading channel has a large memory, the input-output relationship becomes non-linear, and hence, the accuracy of the LMMSE estimator is degraded. Hence, the conventional MMSE estimator

is no longer optimal for estimating signals transmitted over the time-correlated fading channels of the IIoT networks, even when the source signal is Gaussian. An optimal signal estimator in this context, similar to the Bahl-Cocke-Jelinek-Raviv (BCJR) algorithm proposed in [20], can exploit temporal correlation among the signals received over consecutive time slots. However, its computational complexity is exponentially increased with the transmitted frame length, making it infeasible for practical IIoT networks. To strike a suitable balance between computational complexity and detection accuracy, we, therefore, propose a DL-based estimation approach. The main motivation behind such a DL-based estimator is that it can effectively estimate/predict the channel fading state from a set of received I/Q samples by exploiting correlation among them, and thereby, can leverage the LMMSE estimator to infer the transmitted signal for the estimated/predicted channel fading states. Such an approach provides near-optimal and computationally efficient sub-optimal signal estimation when different channel fading states take only different discrete values and different fading distributions, respectively.

The key novelty of this work is that it investigates how to accurately estimate Gaussian source signals in the presence of time-correlated fading channels in IIoT networks. Note that the problems of estimating the channel fading state and transmitted signals are coupled with each other. The joint estimation of fading channel states and the transmitted signals is a nontrivial problem. To the best of our knowledge, our proposed DL approach is the first to tackle the problem of estimating channel fading states and Gaussian source signals in a temporally correlated fading environment of IIoT networks. The threefold contributions of this work are summarized as follows.

- The key challenge of the problem is that we need to estimate both channel fading states and the transmitted signal simultaneously. The precise estimation of the signal is critically dependent on the accurate estimation of the channel fading states. Hence, we propose a two-step approach, where we first accurately estimate the channel fading states and subsequently apply the LMMSE approach to estimate the signal.
- We propose two DL-aided methods to tackle the problem of channel fading states estimation, and, thereby, source signal estimation for the learned channel fading states. The two proposed methods are applicable to different industry applications based on system requirements. Specifically, the first method is capable of directly estimating fading channel states and transmitted signals without any pilot signal transmission at the cost of sub-optimal estimation accuracy. In contrast, the second method is efficient in estimating fading channel states along with transmitted signals with high accuracy, at the expense of utilizing a few time slots for pilot signal transmission.
- In IIoT networks, typically less computationally complex and low-power communication solutions are preferred for sensor-to-sensor information exchange. Taking into account this requirement, we aim to integrate three different standard DNNs, namely long short-term memory (LSTM) [23], temporal convolutional network

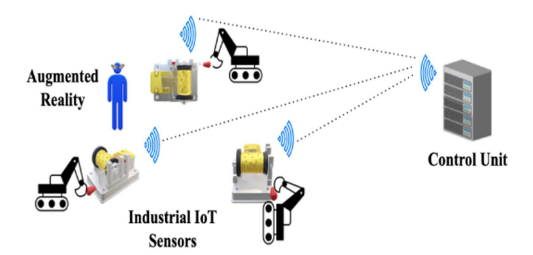


Fig. 1. Industrial IoT Systems.

(TCN) [24], and fully connected DNN. The considered neural network (NN) models are trained offline using the training data sets obtained by the Monte Carlo simulation framework designed for the IIoT system model. Moreover, we tuned the hyperparameters of the respective DL models to render optimal performance in the considered scenario. These trained DNNs are then applied for the estimation of channel fading states online, followed by the estimation of LMMSE-aided source signals. Simulation results demonstrate that the superior performance of the proposed data-driven approaches exhibits a reasonable performance gap from the genie-aided channel estimation scheme that considers perfect knowledge of channel fading states.

The rest of the paper is organized as follows. Section II describes the system model and MMSE estimation process in detail. In Section III, the proposed DL methods are highlighted including model architectures. Simulation results are shown in Section IV. Finally, Section V concludes the paper.

### II. SYSTEM MODEL

### A. Signal Model

In Fig. 1, we consider a point-to-point communication system in an IIoT network, where sensor devices transmit the collected parameters to a control unit (CU) for further processing and decision-making assuming the transmitted signal is impaired by temporally-correlated and frequency-flat fading channels. Let  $s_m$  be the signal transmitted by the sensor node that needs to be estimated by CU during the m-th time slot,  $m \in \{1, 2, \cdots\}$ . We consider that  $s_m$  is drawn from a Gaussian distribution with zero-mean and variance  $\sigma_s^2$ . The signal received at CU during the m-th time slot is represented as

$$y_m = e^{-j\theta_{R,m}} h_m s_m e^{j\theta_{T,m}} + n_m, \tag{1}$$

where  $h_m$  denotes the channel fading gain at the m-th time slot and  $n_m$  presents the additive white Gaussian noise (AWGN) with variance  $\sigma_n^2$ . Moreover,  $\theta_{T,m} \in [0,2\pi]$  and  $\theta_{R,m} \in [0,2\pi]$  represent the phase noises at the transmitter and receiver during the m-th time slot, respectively. The probability density function (PDF) of  $h_m$  is described by a mixture of a finite number of statistical distributions [4], [5]. In particular, the PDF of the random variable  $h_m$ ,  $\forall m$ , is expressed by  $\mathcal{P}_H(h_m;\phi) = \sum_{c=1}^C \rho_c \mathcal{P}_c(h_m;\theta_c)$ , where  $\mathcal{P}_c(\cdot;\theta_c)$  is the c-th component PDF parameterized by  $\theta_c$ ,  $\forall c \in \{1,2,\ldots,C\}$ ;  $C \geq 1$  is the total number of the component PDFs;  $\{\rho_c\}$  is the mixing probabilities

with  $\sum_{c=1}^{C} \rho_c = 1$ ; and  $\phi = \{\theta_1, \dots, \theta_C\}$  is the collection of the fading distribution parameters of all the component PDFs. In an industrial environment, the component PDFs are usually modeled by Gaussian [5, eq. (3)], Gamma [5, eq. (5)], or Gamma-Lognormal [5, eq. (6)] distributions. However, our proposed framework is applicable to other statistical distributions as well. The temporal variation of the fading channel over different time slots is described by a Markov chain, whose states and stationary state distribution are represented by the component fading distributions and the mixing probabilities, respectively [25]-[27]. The switching dynamics among different states or fading distributions are controlled by a transition matrix,  $T_f$ , given by (2) shown at the bottom of this page. In  $\mathbf{T}_f$ ,  $\zeta \in (0,1)$  controls the correlation among fading states observed at the consecutive time slots. Particularly, large values of  $\zeta$  represent persistent fading memory or burst-fading, where several consecutive time slots exhibit identical fading states. In contrast, the fading channel has no memory when  $\zeta = 0$ , and thus, the channel fading states are independently varied over different time slots. The correlation factor can be calculated statistically from a reasonably long time frame for a given network configuration. In particular, the correlation factor  $\zeta$  can be mathematically written as  $\zeta = \lim_{N \to \infty} \sum_{t=1}^{N} x_t/N$ , where

$$x_t = \begin{cases} 1 & \text{for identical states at t-th and (t-1)-th time instants} \\ 0 & \text{otherwise}. \end{cases}$$

We formulate  $\mathbf{T}_f$ , given in (2), such that the steady-state probabilities of the Markov chain become  $\{\rho_1, \rho_2, \dots, \rho_C\}$ . In other words, for any value of  $\zeta \in (0, 1)$ , if we solve  $\pi T_f = \pi$ , we will obtain  $\pi = [\rho_1, \rho_2, \dots, \rho_C]^T$ .

## B. Linear MMSE Estimation of $s_m$

In this section, for a given observation  $y_m$ , we develop an expression for the MMSE optimal Bayesian estimator (OBE) of  $s_m$ . Inspired from [20], [19] the MMSE OBE is obtained as the posterior mean,  $\hat{s}_m(y_m)$  and defined as

$$\hat{s}_m = \mathbb{E}\left[s_m|y_m\right] = \mathbb{E}\left[\mathbb{E}\left[s_m|h_m = c\right]|y_m\right]$$

$$= \sum_{i=1}^{C} \Pr\left(h_m = c|y_m\right) \hat{s}_c^{(m)}(y_m),$$
(3)

where  $\Pr(h_m = c | y_m)$  represents the prior probability of fading channels being in the c-th fading state,  $c \in \{1, 2, \dots, C\}$ ,  $\mathbb{E}\{\cdot\}$  represents statistical expectation, and  $\hat{s}_c^{(m)}(y_m)$  denotes the MMSE detection of  $s_m$  conditioned on  $y_m$  for the channel fading state c. Since  $s_m$  is Gaussian distributed, we can leverage the LMMSE approach to estimate  $s_m$  from  $y_m$  in a computationally efficient manner for the given channel fading state [20], [19]. The

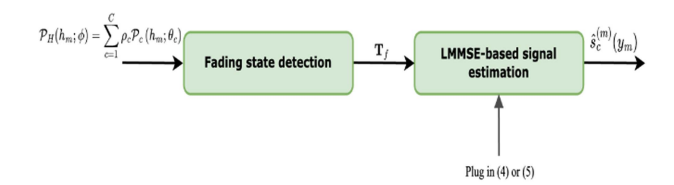


Fig. 2. Proposed two-step estimation approach.

LMMSE of  $\hat{s}_c^{(m)}(y_m)$  by minimizing the MSE is obtained as

$$\hat{s}_{c}^{(m)}(y_{m}) = \frac{\operatorname{Cov}(s_{m}, y_{m})}{\operatorname{Var}(y_{m})} \bar{y}_{m}$$

$$= \frac{\sigma_{s}^{2} \mathbb{E}[|h_{m}|]}{\sigma_{s}^{2} \mathbb{E}[|h_{m}|^{2}] + \sigma_{n}^{2}} \bar{y}_{m}$$
(4)

where  $\bar{y}_m = y_m e^{j\hat{\theta}_{R,m}} e^{-j\hat{\theta}_{T,m}}$ ,  $\mathbb{E}[|h_m|]$  and  $\mathbb{E}[h_m^2]$  represent the first and second order moment of the fading gain at the c-th fading state, respectively. Meanwhile, when different fading states take different deterministic or fixed channel gains, the LMMSE of  $\hat{s}_c^{(m)}(y_m)$  is further simplified as

$$\hat{s}_{c}^{(m)}(y_{m}) = \frac{\sigma_{s}^{2}}{\sigma_{s}^{2} + \frac{\sigma_{n}^{2}}{|h_{m}|^{2}}} \bar{y}_{m}/|h_{m}|.$$
 (5)

Here,  $\hat{\theta}_{T,m} \in [0, 2\pi]$  and  $\hat{\theta}_{R,m} \in [0, 2\pi]$  represent the estimated phase noises at the transmitter and receiver during the m-th time-slot, respectively. It is assumed that the phase noise at the receiver is effectively compensated before the signal estimation stage by leveraging the standard phase noise compensation scheme [28]. The considered LMMSE scheme yields optimal performance when the underlying noise is Gaussian. For IIoT systems impaired by non-Gaussian noise, e.g., impulsive noise, Laplacian noise, unfaded co-channel interference, etc., further investigations are required to obtain the optimal MMSE scheme to estimate Gaussian-distributed signal. It is noteworthy that the accuracy of source estimation by directly plugging (4) or (5) to (3) is degraded when the underlying fading channel has a large memory. However, given that a precise knowledge of the channel fading states is available, a computationally efficient sub-optimal estimation of the source signal is obtained by leveraging (4) when different fading states take different statistical distributions. Furthermore, when different fading states take different deterministic or fixed channel gains, both  $s_m$  and  $y_m$ become jointly Gaussian. In this context, the optimal estimation of  $s_m$  in the MSE sense is directly obtained using (5). Motivated by such a fact, we propose a two-step estimation approach, as depicted in Fig. 2. In our proposed framework, an MMSE OBE can be constructed by first accurately estimating the fading states

$$\mathbf{T}_{f} = \begin{bmatrix} \zeta + (1 - \zeta)\rho_{1} & (1 - \zeta)\rho_{2} & (1 - \zeta)\rho_{3} & \cdots & (1 - \zeta)\rho_{C} \\ (1 - \zeta)\rho_{1} & \zeta + (1 - \zeta)\rho_{2} & (1 - \zeta)\rho_{3} & \cdots & (1 - \zeta)\rho_{C} \\ \vdots & \vdots & \vdots & \vdots & \vdots \\ (1 - \zeta)\rho_{1} & (1 - \zeta)\rho_{2} & (1 - \zeta)\rho_{3} & \cdots & \zeta + (1 - \zeta)\rho_{C} \end{bmatrix}$$
(2)

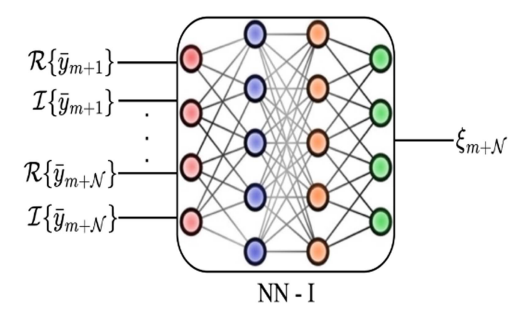


Fig. 3. Neural network for proposed method I.

from the received I/Q samples and then plugging either (4) or (5) for the estimated channel fading states to estimate the transmitted signals. Although a methodology to estimate the state of the Markov channel was proposed in [20], the complexity of such a methodology is significantly increased with the frame sizes and thus lacks scalability. To overcome this challenge, in the next section, we propose data-driven approaches to estimate the fading channel states while exploiting their inherent memory.

# III. PROPOSED DL APPROACHES FOR LMMSE ESTIMATION

### A. Method I: Combined Channel and Signal Estimation

In this method, we develop a DNN model, consisting of an input layer, multiple hidden layers, and a regression output layer, to estimate fading channel states from the received I/Q data samples. Fig. 3 represents the neural network (NN) architecture, denoted by NN-I for the proposed method I.

Offline Training and Online Estimation: Refer to Fig. 3, the input features of NN-I are the  $\mathcal{R}\{\bar{y}_m\}$  and  $\mathcal{I}\{\bar{y}_m\}$ , where  $\mathcal{R}$  and  $\mathcal{I}$ denote the real and imaginary parts of a complex variable respectively. The output labels for NN-I are the memory states of the fading channel represented as  $\xi_m \in \{1, 2, \dots, C\}$  as depicted in Fig. 3. We consider that the fading channel possesses finite states with deterministic values (channel impulse response) for a given state. Therefore, detecting the memory state of the channel in a given time slot is sufficient to obtain the channel state information. As we developed a data-driven approach for detecting the channel state (Methods I and II), the outputs of the designed NNs represent the state of the channels. Since we separate the real and imaginary parts of  $y_m$  and consider them as separate input features for all the realizations of the dataset, therefore, the ultimate dimension of the input features is  $2\mathcal{N}$ . While training for a given (input) feature dimension  $2\mathcal{N}$ , the input variables are denoted as  $[\mathcal{R}\{\bar{y}_{m+1}\}, \mathcal{I}\{\bar{y}_{m+1}\}, \dots, \mathcal{R}\{\bar{y}_{m+\mathcal{N}}\}, \mathcal{I}\{\bar{y}_{m+\mathcal{N}}\}],$ whereas the corresponding output variable is represented as  $\xi_{m+\mathcal{N}}$ . This arrangement of input-output training sequences helps to learn the signal correlation across multiple time slots, thereby assisting in predicting the channel fading state of subsequent time slots. NN-I is trained over a large dataset containing a wide range of signal-to-noise ratios (SNR) to address different use cases of the considered IIoT environments. Once trained, the inference model is deployed at the receiver during real-time data reception. For a given time slot  $m \in \{1, 2, \dots\}$ ,

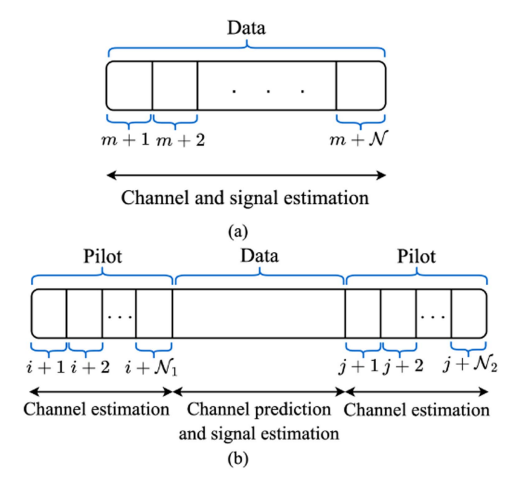


Fig. 4. Time slots specifications in the (a) proposed method I and (b) proposed method II.

the trained NN-I model first predicts  $\hat{\xi}_m$  from a set of received signals  $[\bar{y}_{m-N+1}, \dots, \bar{y}_m]$ , and thereafter estimates  $\hat{s}_m$  using (4) and (5).

# B. Method II: Pilot-Assisted Channel Estimation and Prediction and Signal Estimation

The method of estimating channel fading states and signals in Method I offers improved bandwidth utilization by utilizing all-time slots for data transmission. However, our simulations show that Method I exhibits reduced accuracy in estimating channel fading states from the received I/Q symbols. Note that certain applications in IIoT networks, such as monitoring the temperature and humidity of the system, do not require stringent latency and data transmission accuracy [29]. The proposed Method I is useful for such applications while conservatively using the available bandwidth. To overcome the limitations of the proposed method I for certain IIoT applications, where high accuracy in noisy channel state prediction and signal estimation is essential, we propose method II by leveraging the benefits of using the pilot signals for fading channel estimation. More specifically, as shown in Fig. 4, we divide the entire time horizon into pilot and data transmission phases. The consecutive time slot allocation for the pilot signal facilitates to capture of the temporal correlation of the underlying fading channels efficiently.

Method II estimates the channel fading states during the pilot signal transmission phase and predicts the channel fading states in the data transmission phase by utilizing the estimated channel states. Thereafter, Method II estimates the source signal by plugging the predicted channel states to (4) and (5). The proposed method II contains two stages of the NN models, NN-IIa and NN-IIb, as shown in Fig. 5, and they are utilized for channel fading state estimation and prediction in the pilot and data transmission phases, respectively.

Offline Training of NN-IIa and NN-IIb and Online Estimation and Prediction: The input features of NN-IIa for channel state estimation are  $\mathcal{R}\{\bar{y}_m\}$  and  $\mathcal{I}\{\bar{y}_m\}$ , and the output

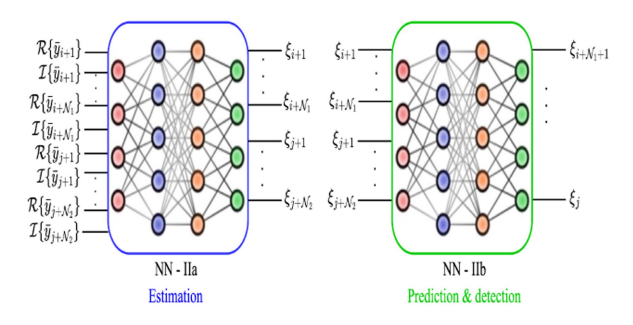


Fig. 5. Neural networks for proposed method II.

labels are the estimated fading channel memory states  $\xi_m$ . The input parameter sequences are expressed as  $[\mathcal{R}\{\bar{y}_{i+1}\}]$ ,  $\mathcal{I}\{\bar{y}_{i+1}\},\ldots,\mathcal{R}\{\bar{y}_{i+\mathcal{N}_1}\},\mathcal{I}\{\bar{y}_{i+\mathcal{N}_1}\},\mathcal{R}\{\bar{y}_{j+1}\},\mathcal{I}\{\bar{y}_{j+1}\},\ldots,$  $\mathcal{R}\{\bar{y}_{j+\mathcal{N}_2}\}, \mathcal{I}\{\bar{y}_{j+\mathcal{N}_2}\}\]$ , and the corresponding output parameter sequences as  $[\xi_{i+1}, \dots, \xi_{\mathcal{N}_1}, \xi_{j+1}, \dots, \xi_{\mathcal{N}_2}]$ . Here,  $\mathcal{N}_1$  and  $\mathcal{N}_2$ represent the dimensions of the first and second sequences of pilot signals, respectively, and  $2(N_1 + N_2)$  denotes the input feature dimension of the estimation model NN-IIa during the offline training phase. Moreover,  $j > i + \mathcal{N}_1 - \mathcal{N}_D - 1$  needs to be satisfied for a successful implementation of NN-IIa and NN-IIb, where  $\mathcal{N}_D$  represents the number of data containing time slots. The input parameter sequences for NN-IIb are represented as  $[\xi_{i+1}, \dots \xi_{i+\mathcal{N}_1}, \xi_{j+1}, \dots \xi_{j+\mathcal{N}_1}]$ . The output parameter sequence is  $[\xi_{i+\mathcal{N}_1+1},\ldots,\xi_j]$ . It is worth mentioning that NN-IIa and NN-IIb can be trained simultaneously and independently to accelerate the offline training phase while leveraging off-the-shelf DNN configuration. While designing custom DNNs by exploiting special structures of signals in the HoT network is expected to improve training and inference accuracy [30], such a task is beyond the scope of this paper and will be considered in our future work. The trained NN-IIa and NN-IIb are deployed at the receiver for online inference.

The proposed two methods reveal insights into addressing the inherent trade-off between bandwidth efficiency and channel fading state prediction accuracy in the presence of time-correlated channel fading. In particular, the proposed DL Method I performs the estimation of channel fading states and subsequently the estimation of source signals without the need for pilots, resulting in high bandwidth efficiency as it utilizes all time slots for data transmission. However, it exhibits a certain degradation in channel fading state prediction accuracy. On the other hand, DL Method II significantly enhances channel fading state prediction accuracy by utilizing a small number of pilot I/Q symbols. Therefore, it is essential to emphasize that the selection of a specific method depends on the requirements of the applications. For example, Method I may be suitable for applications like condition monitoring (e.g., temperature, humidity, vibration measurement using sensors) in an industrial environment [29]. These applications typically do not have stringent latency and data transmission accuracy requirements, allowing Method I to be used while conservatively utilizing available bandwidth. On the other hand, several practical IIoT applications, such as controlling robots through numerous sensors, require both

improved bandwidth utilization and high transmission accuracy. For these applications, Method II is an excellent choice as it strikes a balance between bandwidth/resource utilization and high transmission accuracy by selecting an appropriate number of time slots for pilot transmission. On the other hand, to ensure energy-efficient computation, we assume advanced computing techniques such as neuromorphic engineering [31] will be incorporated while implementing the proposed DNN-aided methods as well as to make it feasible for massive multi-modal sensors equipped IIoT networks in Industry 5.0.

### C. Computational Complexity

The offline training complexity of the proposed methods depends on the complexity of matrix multiplication for both forward and backward propagation in the considered NNs. Without loss of generality, we denote the number of epochs, number of batches per epoch, total number of hidden layers, and number of neurons at the g-th hidden layer in the considered NNs by U, V, G, and  $M_q, g \in \{1, 2, ..., G\}$ , respectively. We also denote the dimension of input features and output labels of such NN by I and O, respectively. The computational complexity for the offline training phase is therefore obtained as  $\mathcal{O}(2(M_1I + M_GO + \sum_{g=1}^{G-1} M_gM_{g+1})VU)$ . Note that  $I = 2\mathcal{N}$  and O = 1 for NN-I;  $I = 2(\mathcal{N}_1 + \mathcal{N}_2)$  and O = 1 $\mathcal{N}_1 + \mathcal{N}_2$  for NN-IIa; and  $I = \mathcal{N}_1 + \mathcal{N}_2$  and  $O = \mathcal{N}_D$  for NN-IIb. Meanwhile, the computational complexity during testing or the real-time communications phase depends on only the forward propagation. Accordingly, the online testing computational complexity of the proposed methods is obtained as  $\mathcal{O}(M_1I +$  $M_GO + \sum_{g=1}^{G-1} M_g M_{g+1}$ ). The proposed DNN-aided methods show polynomial run-time computational complexity, which is directly proportional to energy efficiency. Therefore, using the proposed fully connected feed-forward DNN-aided algorithms will result in relatively less computation compared to conventional signal processing-based approaches, which usually incur high computational complexity for estimating the channel correlation matrix and subsequent processing.

## IV. SIMULATION RESULTS

### A. DL Models Architecture

In the simulations, we employ two different DNN configurations (LSTM and fully Connected DNN model) for the proposed method I and three different DNN configurations (LSTM, TCN, and fully Connected DNN model) for the proposed method II. A more detailed description of these DNN configurations is given as follows.

1) Long Short-Term Memory (LSTM): The LTSM NN-I model consists of multiple hidden layers for the proposed method I. The first hidden layer is the LSTM layer, which is followed by two fully connected hidden layers. All the hidden layers are comprised of the same number of neurons. In the case of proposed method II, the first hidden layer is the bidirectional LSTM layer, as we take two batches of input and predict channel states for the time slots between these input batches for the

prediction stage. Three more fully connected hidden layers are followed by the final output regression layer.

- 2) Temporal Convolutional Network (TCN): For the proposed method II, after the sequential input layer, five hidden layers of the single-dimensional convolutional (Conv1D) layer are specified with different filter numbers and kernel sizes. Each layer is followed by batch normalization and a rectified linear unit (ReLU) layer. The final layer is the output regression layer.
- 3) Fully Connected DNN: The fully connected DNN model consists of a sequential input layer, three hidden layers, and a final output regression layer.

### B. Baseline Schemes

We consider the following two baseline schemes.

- 1) Genie-Aided Scheme: Genie-aided scheme optimally estimates the source signal while considering the availability of perfect channel fading state information for all future time slots. Essentially, this scheme provides the theoretically achievable upper (lower) bound of the estimation accuracy (error).
- 2) Random Prediction Scheme: This scheme randomly selects the channel fading states using a uniform distribution and applies LMMSE estimation for the selected fading state to estimate the input signal. This naive scheme has the lowest computational complexity compared to any model.

### C. Numerical Performance Evaluations

In this subsection, we present the numerical results for the proposed DL-based MMSE schemes to evaluate their performances and compare them with the considered baseline schemes. We show the accuracy of predicting the fading channel states over the considered range of signal-to-noise ratio (SNR), defined as  $\gamma = \sigma_s^2 \mathbb{E}\{|h_m^2|\}/\sigma_n^2$  for the proposed DL-based approaches and the considered baseline schemes. In addition, we compare the performance of the proposed DL-based schemes with baseline approaches in terms of normalized mean square error (NMSE), defined as, NMSE =  $\mathbb{E}\left\{\frac{||Q-\hat{Q}||^2}{||Q||^2}\right\}$ . Here,  $Q \in \{s_m\}$ and  $\hat{\mathcal{Q}} \in \{\hat{s}_m\}$  represent the actual and the estimated input signals respectively. Since we are estimating a signal with an infinite number of possible values, thus the NMSE is the most appropriate choice to be adopted as a performance metric to compare the performance of the proposed scheme with the baseline schemes.

The dataset generation, training, and testing are executed using MATLAB DL toolbox via Monte Carlo simulations. We generate 80,000 realizations of random data samples for training and 20,000 realizations for testing purposes for both the proposed and baseline schemes. For the considered simulation results, we assume  $\mathcal{N}=20$  and initialize m unless otherwise stated. Moreover, the fading channels possess two states (state 1 and state 2), and the corresponding gain of channels is set as  $|h_1|=3$  and  $|h_2|=5$ , respectively. In case of proposed method II, we assume  $\mathcal{N}_1=3$  and  $\mathcal{N}_2=3$ , and set i=0 and j=17 for the initial batch. We then increase i and j by  $\mathcal{N}_1+\mathcal{N}_D+\mathcal{N}_2$  in subsequent batches for training. In this work, we consider the

TABLE I NMSE PERFORMANCES OF PROPOSED METHOD I

SNR	NMSE	NMSE	NMSE	NMSE (Lever-
	(Genie)	(LSTM)	(DNN)	aging [19])
-20dB	0.4641	0.4663	0.4663	0.4510
-10dB	0.0839	0.1373	0.1664	0.4603
0dB	0.0092	0.0881	0.1273	0.4555
10dB	0.0029	0.0856	0.1226	0.4788
20dB	0.0009	0.0813	0.1202	0.4639

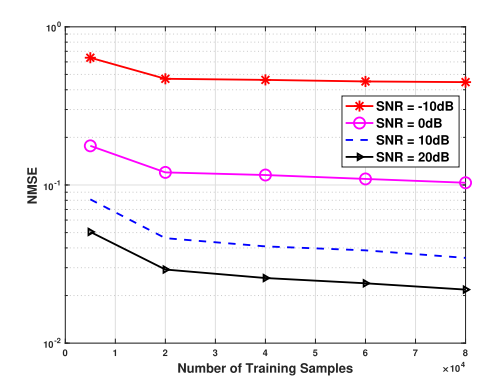


Fig. 6. Neural network training impact on NMSE in method II.

same environment for training and testing while conducting simulations for experiments. In the practical environment, if there are notable changes in the operating environment that impact data transmission, underlying channel, and noise impairment, we need to retrain the model to obtain a better performance.

Performance Analysis of Proposed Method I: Table I shows the comparison of NMSE as a function of SNR  $\gamma$  for the Genieaided scheme, LSTM, and fully connected DNN configurations for the proposed method I. Moreover, we leverage the trained model proposed in [19] to detect the channel states and show the corresponding NMSE. It is evident that the inference model from [19] completely fails to predict the channel states and hence, it does not provide improved NMSE even at high SNRs. Meanwhile, the LSTM and fully connected DNN models give channel states an average prediction accuracy of approximately 80% and 72%, respectively. Since the difference of deterministic channel gain between two fading states of the channel is high, a small percent of incorrect detection of (channel) states significantly raises the NMSE for estimating the input signal. Moreover, without any prior knowledge of the input signal, detecting channel states with high accuracy by learning only from the received signal is not easy, even if the sophisticated DL model is chosen. Therefore, the proposed method I yields a sub-optimal NMSE performance. Nevertheless, compared to method II, method I can transmit more data symbols in the given time slots as it does not require the transmission of known pilot signals for channel estimation, and thus, can be useful in applications without stringent estimation accuracy requirements.

Training Impacts on NMSE in the Proposed Method II: In Fig. 6, we illustrate the impacts of the neural network training samples on NMSE over a range of SNR in the proposed method II. We consider several configurations of training parameters by

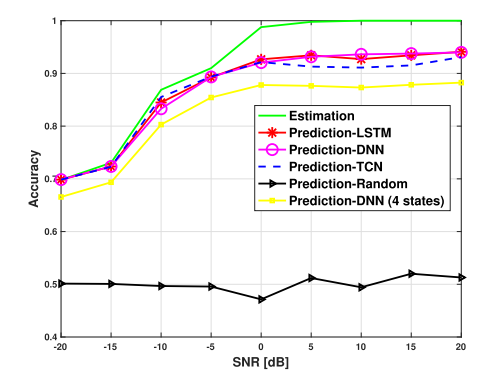


Fig. 7. Estimation and prediction accuracy in method II.

tuning the size of training datasets. It is obvious that increasing SNR for different training datasets decreases the NMSE. As the data size increases from 5,000 to 20,000, the NMSE is decreased by approximately 64% for the considered SNRs. Moreover, in the case of -10 dB SNR, increasing the size of datasets by more than 20,000 does not reduce NMSE significantly, whereas, for 20 dB SNR, the performance still improves for dataset size beyond 60,000. It is worth pointing out that increasing the number of datasets increases the training computations. Hence, depending on the system parameters, e.g., SNR, it is imperative to carefully tune the cardinality of the training dataset.

Comparison Among Proposed Schemes and Baseline Schemes: Fig. 7 plots the channel fading states estimation and prediction accuracy of the proposed Method II. Recall that estimation and prediction of the channel fading states are performed during the pilot and data transmission phases, respectively. We observe that the channel fading state estimation accuracy sharply increases from 85% in the low SNR region (-10 dB) to 100% in high SNR (5 dB onward) corresponding to the pilot transmission slots. Meanwhile, the accuracy of channel fading state prediction initially increases with SNR and remains around  $\sim 94\%$  for SNR equal to or greater than 0 dB corresponding to the data transmission slots. Moreover, channel fading state prediction accuracy of different neural network architectures, such as LSTM and fully connected DNN are almost the same whereas the TCN model's accuracy is slightly degraded at high SNRs. The random state prediction scheme shows an average 50% prediction accuracy, which is expected for two states fading channels. We also observe that at the high SNR region, prediction accuracy is decreased from 94% to 87% when the number of channel fading states is increased from two to four. It is worth noting that for both two and four fading states of the channel, we considered the same number of slots for pilot-based channel fading estimation. Essentially, in order to obtain higher accuracy for channel fading state prediction for a large number of fading states, one needs to enhance the slots of pilot signal transmission to exploit the temporal correlation more accurately. HoT networks exhibit a hostile communication environment due to interference from nearby radio devices, reflection from metallic objects, frequent movement of objects, etc., that result in temporally correlated fading channels. The classical channel

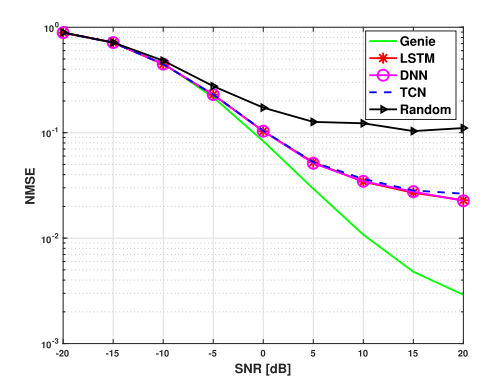


Fig. 8. Estimation error in method II.

estimation algorithms fail to provide optimal signal detection and channel estimation in such IIoT environments because of inaccurate estimation of temporally correlated fading channel states. Moreover, as the number of fading channel states increases, the complexity of accurately estimating channel states increases exponentially while using classical channel estimation techniques because of computing the inverse of correlation matrices of underlying channels [20]. Unlike the classical channel estimation approaches, the DL approaches can exploit the time-correlation structure of channel fading with memory. Moreover, the DL method is computationally efficient for the fading channel with a large number of fading states since the computational complexity of a DL approach increases linearly with the number of hidden layers. Hence, we conclude that the DL-aided approaches can provide near-optimal solutions in estimating fading channel memory states and estimation of transmitted signals with less complexity compared to classical estimation techniques in the considered scenario.

In Fig. 8, we compare the NMSE performance of the proposed and baseline schemes. We observe that the proposed schemes achieve negligible NMSE performance loss from the genie-aided estimation scheme for SNR <=0 dB. However, the relative performance gaps between the genie-aided scheme and our proposed scheme increase as the SNR increases beyond 0 dB. It is also evident that a fully connected DNN scheme provides similar performance to the LSTM and TCN schemes. As expected, all the proposed schemes significantly improved NMSE compared to the naive random-selection scheme in the high SNR regimes.

Fig. 9 illustrates the effectiveness of estimating signal using our proposed methods applying (5) compared to (3). It is obvious that the NMSE is notably high when the standard MMSE OBE in (3) is used for signal estimation. This clearly supports the fact that the conventional LMMSE approach is no longer effective in estimating source signals in the presence of time-correlated channel fading. In contrast, by adding a fading state detection step prior to the signal estimation step, our proposed two-step approach can estimate the signal with a significantly lower error rate over the entire region of SNR.

Fig. 10 demonstrates the impact of channel correlation factor  $\zeta$  on the NMSE performance for the proposed fully-connected

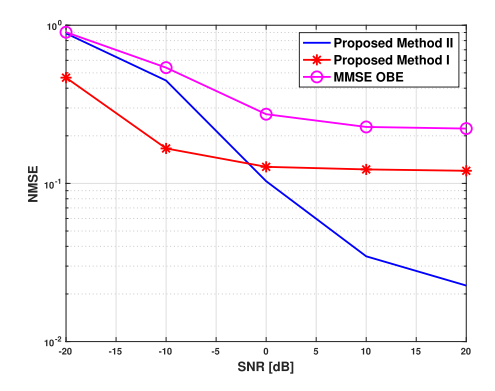


Fig. 9. Effectiveness of the proposed approach.

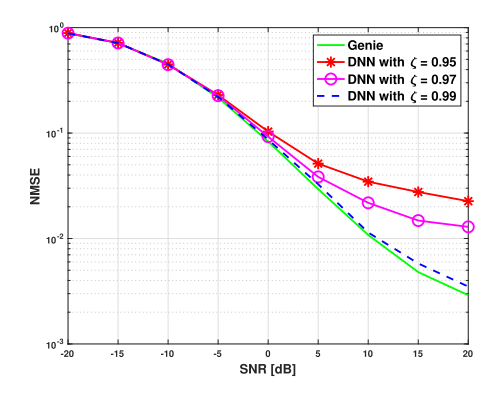


Fig. 10. Estimation error for different channel correlation factors.

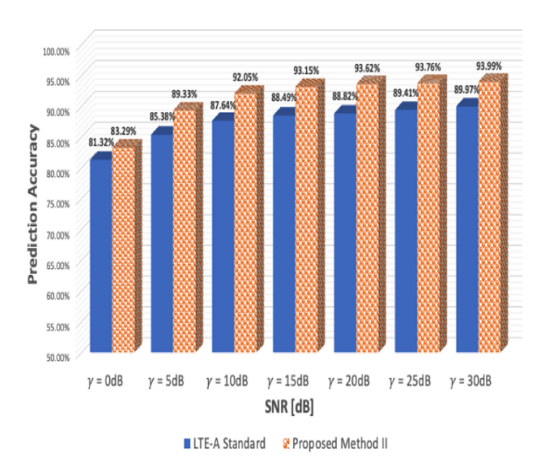


Fig. 11. Prediction accuracy comparison.

DNN estimation scheme. We observe that the NMSE performance gap between the genie-aided and DNN-based estimation schemes decreases significantly for increasing  $\zeta$ . As  $\zeta$  gets closer to 1, the estimation error of DL models becomes closer to the genie-aided estimation at the high SNR region. This finding reflects the effectiveness of our proposed scheme in estimating the correct channel state for highly correlated channels.

In Fig. 11, we show the accuracy of the prediction of the channel fading state in the data transmission slots for two

scenarios. Scenario 1 considers the time-slot specification strategy deployed in our simulation model (used for Method II), whereas Scenario 2 adopts the numerology from the long-term evolution advanced (LTE-A) scheme. It is to be noted that the LTE-A standard allocates slots for pilot transmission in a specific arrangement (e.g. orthogonal frequency division multiplexing (OFDM) symbols 1, 5, 9, 13, 17 for each subframe). Fig. 11 shows that our proposed time slot specification for Method II can predict channel fading states with higher accuracy than the LTE-A compatible time slot specification. Thus, to capture time correlation efficiently, it is rational to allocate consecutive time slots for pilot signals for channel estimation rather than in a non-consecutive manner. Since the considered system model and the proposed methods are applicable to the IIoT environment, which is usually a production or manufacturing industry's indoor environment equipped with a plethora of smart sensors, therefore the operating spectrum of communications will take place typically in an unlicensed industrial, scientific, and medical (ISM) band. In this context, we can use suitable time slot specifications for the pilot signal and actual data transmission of ISM-band standards that facilitate the accuracy and reliability of the data transmission scheme. A notable advantage of the proposed Method II is that it can select the number of time slots in the pilot transmission phase for channel fading state estimation. Therefore, the proposed Method II can strike a suitable balance among different factors, namely, bandwidth utilization, accuracy, and protocol compatibility, by selecting a suitable number of time slots for pilot transmission.

### V. CONCLUSION

We proposed two data-driven approaches for estimating the Gaussian source subjected to temporally correlated fading channels in the IIoT environment. Our proposed schemes exploit the statistical correlation among the consecutive fading channel states while conducting estimation and prediction operations. Although the proposed method I shows sub-optimal performance, it does not require pilot signals and leverages prior data information to predict channels' fading states. In contrast, the proposed method II provides better performance in predicting and estimating channel states by exploiting pilot signals prior to data transmission. We also showed that the fully connected DNN model performs equally well as the LSTM and TCN models in predicting channel fading states and estimating the source signal with high accuracy. The potential future work could be designing custom DNNs while analyzing the specific inherent structure of the signals to obtain higher accuracy in the estimation process.

#### **ACKNOWLEDGMENT**

The authors show their sincere thanks to the funding agencies.

### REFERENCES

- E. Sisinni, A. Saifullah, S. Han, U. Jennehag, and M. Gidlund, "Industrial Internet of Things: Challenges, opportunities, and directions," *IEEE Trans. Ind. Informat.*, vol. 14, no. 11, pp. 4724–4734, Nov. 2018.
- [2] H. Boyes, B. Hallaq, J. Cunningham, and T. Watson, "The Industrial Internet of Things (IIoT): An analysis framework," *Comput. Ind.*, vol. 101, pp. 1–12, 2018.

- [3] F. Brizzi, L. Peppoloni, A. Graziano, E. D. Stefano, C. A. Avizzano, and E. Ruffaldi, "Effects of augmented reality on the performance of teleoperated industrial assembly tasks in a robotic embodiment," *IEEE Tran. Hum.-Mach. Syst.*, vol. 48, no. 2, pp. 197–206, Apr. 2018.
- [4] A. Ahlen et al., "Toward wireless control in industrial process automation: A case study at a paper mill," *IEEE Control Syst. Mag.*, vol. 39, no. 5, pp. 36–57, Oct. 2019.
- [5] T. Olofsson, A. Ahlén, and M. Gidlund, "Modeling of the fading statistics of wireless sensor network channels industrial environments," *IEEE Trans. Sig. Process.*, vo. 64, no. 12, pp. 3021–3034, Jun. 2016.
- [6] Y. Liu, M. Kashef, K. B. Lee, L. Benmohamed, and R. Candell, "Wireless network design for emerging IIoT applications: Reference framework and use cases," *Proc. IEEE*, vol. 107, no. 6, pp. 1166–1192, Jun. 2019.
- [7] M. Wollschlaeger, T. Sauter, and J. Jasperneite, "The future of industrial communication: Automation networks in the era of the Internet of Things and Industry 4.0," *IEEE Ind. Electron. Mag.*, vol. 11, no. 1, pp. 17–27, Mar. 2017.
- [8] H. X. Nguyen, R. Trestian, D. To, and M. Tatipamula, "Digital twin for 5G and beyond," *IEEE Commun. Mag.*, vol. 59, no. 2, pp. 10–15, Feb. 2021.
- [9] O. Chukhno, N. Chukhno, G. Araniti, C. Campolo, A. Iera, and A. Molinaro, "Placement of social digital twins at the edge for beyond 5G IoT networks," *IEEE Internet Things J.*, vol. 9, no. 23, pp. 23927–23940, Dec. 2022.
- [10] K. F. Tsang, M. Gidlund, and J. Åkerberg, "Guest editorial industrial wireless networks: Applications, challenges, and future directions," *IEEE Trans. Ind. Informat.*, vol. 12, no. 2, pp. 755–757, Apr. 2016.
- [11] A. W. Colombo, S. Karnouskos, Y. Shi, S. Yin, and O. Kaynak, "Industrial cyber–physical systems [scanning the issue]," *Proc. IEEE*, vol. 104, no. 5, pp. 899–903, May 2016.
- [12] J. Wan et al., "Software-defined industrial Internet of Things in the context of Industry 4.0," *IEEE Sensors J.*, vol. 16, no. 20, pp. 7373–7380, Oct. 2016
- [13] R. Drath and A. Horch, "Industrie 4.0: Hit or Hype? [Industry Forum]," *IEEE Ind. Electron. Mag.*, vol. 8, no. 2, pp. 56–58, Jun. 2014.
- [14] T. S. Rappaport and C. D. McGillem, "UHF fading in factories," *IEEE J. Sel. Areas Commun.*, vol. 7, no. 1, pp. 40–48, Jan. 1989.
- [15] F. Bouchereau and D. Brady, "Method-of-moments parameter estimation for compound fading processes," *IEEE Trans. Commun.*, vol. 56, no. 2, pp. 166–172, Feb. 2008.
- [16] R. A. Berry and R. G. Gallager, "Communication over fading channels with delay constraints," *IEEE Trans. Inf. Theory*, vol. 48, no. 5, pp. 1135–1149, May 2002.
- [17] P. Agrawal, A. Ahlén, T. Olofsson, and M. Gidlund, "Long term channel characterization for energy efficient transmission in industrial environments," *IEEE Trans. Commun.*, vol. 62, no. 8, pp. 3004–3014, Aug. 2014.
- [18] S. Thoen, L. Van der Perre, and M. Engels, "Modeling the channel time-variance for fixed wireless communications," in *IEEE Commun. Lett.*, vol. 6, no. 8, pp. 331–333, Aug. 2002.
- [19] I. Ahmed, M. S. Alam, M. J. Hossain, and G. Kaddoum, "Deep learning for MMSE estimation of a Gaussian source in the presence of bursty impulsive noise," *IEEE Commun. Lett.*, vol. 25, no. 4, pp. 1211–1215, Apr. 2021.
- [20] M. S. Alam, G. Kaddoum, and B. L. Agba, "Bayesian MMSE estimation of a gaussian source in the presence of bursty impulsive noise," *IEEE Commun. Lett.*, vol. 22, no. 9, pp. 1846–1849, Sep. 2018.
- [21] Y. Li, Y. Pu, C. Cheng, and Q. Xiao, "Scalable Gaussian process for large-scale periodic data," *Technometrics*, vol. 65, pp. 363–374, Jan. 2023, doi: 10.1080/00401706.2023.2166124.
- [22] A. K. Jain, R. P. W. Duin, and J. Mao, "Statistical pattern recognition: A review," *IEEE Trans. Pattern Anal. Mach. Intell.*, vol. 22, no. 1, pp. 4–37, Jan. 2000.
- [23] W. Zhang, M. Feng, M. Krunz, and A. H. Y. Abyaneh, "Signal detection and classification in shared spectrum: A deep learning approach," in *Proc. IEEE Conf. Comput. Commun.*, 2021, pp. 1–10.
- [24] S. Bai et al., "An empirical evaluation of generic convolutional and recurrent networks for sequence modeling," 2018, arXiv:1803.01271.
- [25] D. E. Quevedo, A. Ahlen, and K. H. Johansson, "State estimation over sensor networks with correlated wireless fading channels," *IEEE Trans. Autom. Control*, vol. 58, no. 3, pp. 581–593, Mar. 2013.
- [26] P. S. Castro, "Scalable methods for computing state similarity in deterministic Markov decision processes," in *Proc. AAAI Conf. Artif. Intell.*, 2020, pp. 10069–10076.
- [27] D. E. Quevedo, A. Ahlén, and K. H. Johansson, "Stability of state estimation over sensor networks with Markovian fading channels," in *Proc. IFAC World Congr.*, 2011, pp. 12451–12456.

- [28] A. Mohammadian, C. Tellambura, and G. Y. Li, "Deep learning-based phase noise compensation in multicarrier systems," *IEEE Wireless Commun. Lett.*, vol. 10, no. 10, pp. 2110–2114, Oct. 2021.
- [29] ETSI TR 103 588, "Reconfigurable radio systems (RRS); Feasibility study on temporary spectrum access for local high-quality wireless networks," 2018. [Online]. Available: https://www.etsi.org/deliver/etsi\_tr/ 103500\_103599/103588/01.01.01\_60/tr\_103588v010101p.pdf
- [30] A. Lancho et al., "Data-driven blind synchronization and interference rejection for digital communication signals," in *Proc. IEEE Glob. Commun. Conf.*, 2022, pp. 2296–2302.
- [31] T. Luo et al., "Achieving green AI with energy-efficient deep learning using neuromorphic computing," *Commun. ACM*, vol. 66, no. 7, pp. 52–57, Jul. 2023, doi: 10.1145/3588591.



Majumder Haider (Graduate Student Member, IEEE) received the B.Sc. degree in electronics and communication engineering from BRAC University, Dhaka, Bangladesh, and the M.Sc. degree in electronics and communication systems engineering from the City University of Applied Sciences, Bremen, Germany. He is currently working toward the Ph.D. degree in electrical engineering with Howard University, Washington, DC, USA. His research interests include wireless communication systems design

and optimization applying AI/ML techniques, intelligent reconfigurable surfaces, massive MIMO communications, and industrial IoT networks. He was the recipient of two prestigious graduate fellowships in his Ph.D. studies.



Md. Zoheb Hassan (Member, IEEE) received the doctorate degree from Electrical and Computer Engineering Department, University of British Columbia, Vancouver, BC, Canada. He is currently an Assistant Professor with the Department of Electrical and Computer Engineering, Université Laval, Quebec City, QC, Canada. Prior to joining Université Laval, he was the Senior Postdoctoral Research Fellow with École de technologie Superiéure, Montreal, QC, and Research Assistant Professor with the ECE De-

partment, Virginia Tech, Blacksburg, VA, USA. He authored and coauthored more than 30 journal articles and 15 conference papers in radio resource optimization, interference management, spectrum sharing, and optical wireless communications. He was/is the TPC member of various prestigious IEEE Conferences, like IEEE GLOBECOM, ICC, MILCOM, VTC, and PIMRC and reviewer of several major journals of IEEE Communication Society.



Imtiaz Ahmed (Senior Member, IEEE) received the Ph.D. degree in electrical and computer engineering from The University of British Columbia, Vancouver, BC, Canada. After finishing his Ph.D. degree, he was with Intel Corporation, San Diego, CA, USA, as a Wireless Systems Engineer, and Marshall University, Huntington, WV, USA, as an Assistant Professor. He is currently an Assistant Professor with the Department of Electrical Engineering and Computer Science, Howard University, Wash-

ington, DC, USA. He works in the areas of wireless communications, signal processing, and computer networks. His research interests include artificial intelligence-aided physical layer designs, cell-free communications, integration of aerial and terrestrial communication networks, and communications with THz bands, and intelligent reflecting surfaces.



Jeffrey H. Reed (Life Fellow) is currently the Willis G. Worcester Professor of ECE. He has authored or coauthored more than 500 articles and books. His research interests include wireless communications, wireless security, cognitive radio, software radio, telecommunications policy, and spectrum access. In addition, he cofounded several commercial companies, including Federated Wireless, which commercializes spectrum sharing, PFP Cybersecurity, which provides security solutions for IoT devices, and

Cirrus360, which produces tools for rapid prototyping of O-RAN. He is the Founding Director of Wireless@Virginia Tech, a university research center, and Co-Founder of Virginia Tech's Hume Center for National Security and Technology, where he was the Interim Director. He was also the Interim Director of the Commonwealth Cyber Initiative and is currently its CTO. Dr. Reed is a Life Fellow of the IEEE for contributions to software radio and communications signal processing and for leadership in engineering education.



Danda B. Rawat (Senior Member, IEEE) is currently an Associate Dean for Research and Graduate Studies, a Full Professor with the Department of Electrical Engineering and Computer Science, Founding Director of the Howard University Data Science and Cybersecurity Center and Founding Director of DoD Center of Excellence in Artificial Intelligence & Machine Learning (CoE-AIML), Howard University, Washington, DC, USA. He successfully led and established the Research Institute for Tac-

tical Autonomy (RITA), the 15th University Affiliated Research Center (UARC) of the US Department of Defense as the PI/Founding Executive Director at Howard University, Washington, DC, USA. He has secured over \$110 million as a PI and over \$18 million as a Co-PI in research funding from the US federal agencies (NSF, DHS, DoD NSA, DoE/NNSA, and NIH), Industry (Microsoft, Intel, VMware, PayPal, Mastercard, Meta, BAE, and Raytheon etc.) and private Foundations.



Ahmed Rubaai (Life Fellow) received the M.S.E.E. degree from Case Western Reserve University, Cleveland, OH, USA, and the Dr.Eng. degree from Cleveland State University, Cleveland, OH, in 1983 and 1988, respectively. In 1988, he joined Howard University, Washington, DC, USA, as a Faculty Member, where he is currently a Professor and the Chairperson of the Electrical Engineering and Computer Science Department. His research interests include high performance motor drives and their

related knowledge-based control structure, and development of intelligent applications for manufacturing systems, and industrial applications. Dr. Rubaai was the recipient of the IEEE Industry Applications Society (IAS) 2nd Prize Paper Award in September 2007, ASEE Division of Experimentation and Laboratory Oriented Studies Best Paper Award in June 2006, Howard University Exemplary Teaching Award in April 2005, IEEE IAS Honorable Mention Prize Paper Award in October 2002, NASA Glenn Software Release Award in June 2004, and Howard's School of Engineering "Professor of the Year" in 1997 and 1998. He was the Chair of the IEEE-IAS Publications Department (2012–2018), Chair of the IEEE-IAS Manufacturing Systems Development and Applications Department (2006–2008), Chair of the IAS Industrial Automation and Control Committee (2000–2002), and Chair of ASEE Division of Experimentation and Laboratory Oriented Studies (2010–2011). He has been named an IEEE Fellow in 2015.